One-Pot Formic Acid Dehydrogenation and Synthesis of Benzene-fused Heterocycles over Reusable AgPd/WO2.72 Nanocatalyst

Journal:	*Journal of Materials Chemistry A*
Manuscript ID	TA-ART-09-2018-009342.R1
Article Type:	Paper
Date Submitted by the Author:	02-Nov-2018
Complete List of Authors:	Yu, Chao; Brown University, Chemistry Guo, Xuefeng; Brown University, Chemistry Shen, Bo; Brown University, Chemistry Xi, Zheng; University of Central Florida, Chemistry Li, Qing; Huazhong University of Science and Technology, School of Materials Science and Engineering Yin, zhouyang; Brown University, Chemistry Liu, Hu; Harbin Institute of Technology, School of Chemical Engineering and Technology Muzzio, Michelle; Brown University, Department of Chemistry shen, mengqi; Department of Chemistry, Li, Junrui; Brown University, Chemistry Seto, Christopher; Brown University, Chemistry Sun, Shouheng; Brown University, Chemistry

Journal Name

One-Pot Formic Acid Dehydrogenation and Synthesis of Benzene-fused Heterocycles over Reusable AgPd/WO$_{2.72}$ Nanocatalyst†

Chao Yu,[‡a] Xuefeng Guo,[‡a] Bo Shen,[a] Zheng Xi,[a] Qing Li,[b] Zhouyang Yin,[a] Hu Liu,[a] Michelle Muzzio,[a] Mengqi Shen,[a] Junrui Li,[a] Christopher T. Seto*[a] and Shouheng Sun*[a]

Using nanoparticles (NPs) to catalyze multiple chemical reactions in one-pot and to achieve high-yield syntheses of functional molecules/materials is an important direction in NP chemistry, catalysis and applications. In this article, we report a nanocomposite of AgPd NPs anchored on WO$_{2.72}$ nanorods (NRs) (denoted as AgPd/WO$_{2.72}$) as a general catalyst for formic acid dehydrogenation and transfer hydrogenation from Ar-NO$_2$ to Ar-NH$_2$ that further reacts with aldehydes to form benzene-fused heterocyclic compounds. The AgPd/WO$_{2.72}$ catalysis is Ag/Pd dependent and Ag$_{48}$Pd$_{52}$ is the most active composition for the multiple chemical reactions. The high activity of AgPd/WO$_{2.72}$ arises from strong interfacial interaction between AgPd and WO$_{2.72}$, resulting in AgPd lattice expansion and electron polarization from AgPd to WO$_{2.72}$. The syntheses proceed in one-pot reactions among formic acid, 2-nitrophenol (or 2-nitroaniline, or 2-nitrothiophenol) and aldehydes in dioxane/water (2/1 v/v) at 80-90 °C, leading to one-pot syntheses of benzoxazoles, benzimidazoles and benzothiazoles that are key ring structures present in functional compounds for pharmaceutical, optical and polymer applications.

[a.] Department of Chemistry, Brown University, 324 Brook St. Providence, RI 02912, United States.

[b.] Current Address: School of Materials Science and Engineering, Huazhong University of Science and Technology, Wuhan 430074, China

[‡] These authors contributed equally to this work.

[*] E-mail: ssun@brown.edu, christopher_seto@brown.edu.

1 Introduction

Benzene-fused heterocycles, are common core structures found in compounds prepared for biomedical, sensor and optical applications.[1-5] Some typical examples of these structures are benzoxazoles where X = O, NH or S. Once properly functionalized for polymer formation, the ring structure is also a key component of a class of rigid organic polymers, such as polybenzozaxoles, that are important for ballistic fiber, flame retardant and electronic textile applications.[6-9] Conventional chemistry leading to the synthesis of benzoxazoles often requires long reaction times (up to 24 h), harsh reaction conditions (over 130 °C), reactive additives (H_2O_2), and toxic solvents.[10-14] These conditions can make it challenging to prepare aromatic ring structures with controlled functionalization to tune their chemical and physical properties. Ideally, the synthesis could proceed using a one-pot reaction with easily available precursors in a green chemistry environment without compromising the synthetic yield and selectivity.

Catalytic dehydrogenation of small molecules to release hydrogen (H_2) is an attractive approach to organic hydrogenation reactions without using pure H_2 as a reactant.[15,16] The common H_2 storage materials explored for H_2 formation or hydrogenation reactions include conventional alcohols and hydrides.[17-19] Recently, ammonia borane ($NH_3 \cdot BH_3$) and formic acid (HCOOH) have attracted a lot of attention as H_2 storage materials.[20-30] HCOOH as a H_2 carrier is especially appealing since it is easily available from oxidation of biomass, or hydrogenation of CO_2. Recently, AgPd and AuPd alloy nanoparticles (NPs) were found to be active and stable for HCOOH dehydrogenation into H_2 and CO_2, and to initiate transfer hydrogenation to RNO_2 to give RNH_2.[31-36] Especially when AgPd NPs were coupled to oxygen-deficient $WO_{2.72}$, they catalyzed one-pot reactions among HCOOH, nitrophenol and aldehydes in H_2O/dioxane, providing a clean and safe method for preparing benzoxazoles.[32]

Despite the exciting synthetic potential demonstrated in the AgPd/$WO_{2.72}$ catalyzed one-pot reactions to yield benzoxazoles, there are two questions that remain unanswered: 1) why are these AgPd/$WO_{2.72}$ nanocomposites more active than AgPd NPs (AgPd is still active but with lower efficiency)? 2) can this one-pot strategy be extended to produce other aromatic analogues, as shown in Fig. 1, without significantly changing the reaction conditions? This paper aims to answer these two questions by studying what makes AgPd/$WO_{2.72}$ more active than simpler AgPd NPs, and by demonstrating that the one-pot synthesis can indeed be applied not only to benzoxazoles, but also to other structures where X = NH and S (Fig. 1). The reactions provide a general approach to C-X bond formation and high yield production of benzene-fused heterocyclic compounds.
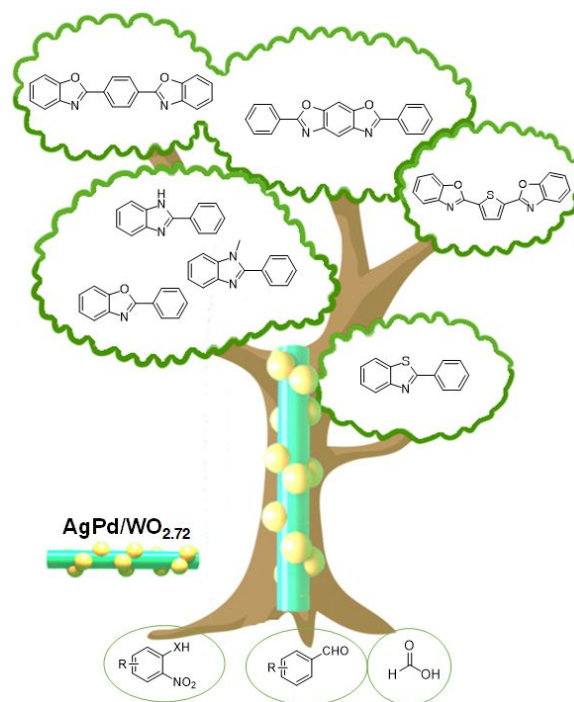

Fig. 1 The schematic illustration of $Ag_{48}Pd_{52}$/$WO_{2.72}$-catalyzed one-pot syntheses of benzoxazoles (where X = O, NH, S).

2 Experimental

2.1 Material

The NP synthesis was carried out using standard airless procedures and commercially available reagents. All reagents were used as received. Oleylamine (OAm, >70%), 1-octadecene (ODE, technical grade, 90%), oleic acid (OA, 90 %), formic acid (FA, 95 %), nitro compounds 2-nitrophenol, 2-nitrothiophenol, 2-nitroaniline and various benzaldehydes were from Sigma-Aldrich. Tungsten (IV) chloride, 97 % (WCl_4), silver (I) acetate (Ag(Ac)$_2$, 97%), and palladium (II) acetylacetonate (Pd(acac)$_2$, 95%) were from Strem Chemicals. 4,6-Dinitroresorcinol was purchased from Fisher Scientific. These chemicals were used without further purification. The deionized water was obtained from a Millipore Autopure System.

2.2 Preparation and characterization

2.2.1 Synthesis of $WO_{2.72}$ NRs

81 mg WCl_4 (0.25 mmol), 5 mL ODE, 3 mL OAm were first mixed in a 20 mL vial through sonication to form a dark brown solution and transferred into a 100 mL four-neck round bottom flask. 10 mL ODE and 6 mL OAc were then added into the flask. The mixture solution was first heated to 120 °C in a gentle Ar flow and magnetic stirring for 30 min to remove air and moisture from the reaction system. The clear dark green solution was then heated to 280 °C in 30 min (when the reaction temperature reached 200 °C, the Ar gas was switched to form an Ar blanket over the reaction system and the solution started to turn to blue). The reaction solution was kept at 280 °C for 10 h before it was cooled to room temperature. The product was separated from the solution by adding 80 mL ethanol and centrifuging at

9500 rpm for 8 min. Then 20 mL hexane was added to re-disperse the synthesized NRs and centrifugation (6000 rpm, 4 min) was applied to precipitate any undispersed material. The product in the dispersion was then precipitated by adding 35 mL ethanol followed by centrifugation. The NRs were purified again with 15 mL hexane and 35 mL ethanol. After separation by centrifugation, the NRs were dispersed in hexane for further use.

2.2.2 Synthesis of AgPd/$WO_{2.72}$ Nanocomposites

Under a gentle nitrogen flow, 0.084 g of Ag(Ac) (0.5 mmol), 0.15 g of Pd(acac)$_2$ (0.5 mmol) and 0.34 g of $WO_{2.72}$ NRs (1.5 mmol) were magnetically stirred in 4.5 mL of OAc, 0.5 mL of OAm, and 10 mL of ODE. The mixture was heated to 80 °C to generate a homogeneous solution and kept for 1 h. Then the solution was heated to 180 °C at a rate of 5–7 °C/min. The reaction was allowed to proceed for 20 min and cooled to room temperature. 100 mL of isopropanol was added, and the product was separated by centrifugation at 9500 rpm for 15 min to remove the organic impurities and precursor residues. The product was redispersed in 10 mL of hexane and then recollected by adding 40 mL of ethanol and centrifugation at 9500 rpm for 8 minutes. The products were washed twice with hexane/ethanol (v/v= 1:15) and then suspended in 30 mL of acetic acid and the suspension was stirred at 60 °C for 10 h. 30 mL of ethanol was added and the mixture was centrifuged at 9500 rpm for 8 minutes. This ethanol washing procedure was repeated for three times, yielding $Ag_{48}Pd_{52}/WO_{2.72}$, which was dispersed in hexane for future use. The composition of AgPd/$WO_{2.72}$ was controlled by the molar ratio of metal precursors. For instance, with the total amount of metal precursor fixed at 1.0 mmol, $Ag_{78}Pd_{22}/WO_{2.72}$, $Ag_{57}Pd_{43}/WO_{2.72}$, $Ag_{48}Pd_{52}/WO_{2.72}$, $Ag_{38}Pd_{61}/WO_{2.72}$ and $Ag_{20}Pd_{80}/WO_{2.72}$ were formed in the molar ratio from 3:1, 2:1, 1:1, 1:2 and 1:3 respectively.

2.2.3 Decomposition of FA

A two-necked reaction flask (25 mL) containing a Teflon-coated stir bar was placed on a magnetic stirrer and thermostated to 50.0 ± 1 °C by using a constant temperature bath. A gas burette filled with water was connected to one neck of the flask (the other neck was sealed) to measure the volume of gas mixture evolved from the reaction. 9.64 mL of aqueous suspension of the catalyst was transferred into the reaction flask, and 0.36 mL (9 mmol) of FA was added into the stirred (800 rpm) solution. The volume of gas mixture evolved was measured by recording the volume of water displaced. The reaction was considered to cease when hydrogen gas generation was no longer observed.

2.2.4 CO_2 Removal from the H_2 and CO_2 Mixture

To quantify the molar ratio of CO_2 to H_2 in the gas mixture generated during the AgPd/$WO_{2.72}$ catalyzed dehydrogenation of aqueous FA solution (10 mL of 900 mM), the gas burette system was modified by placing a NaOH trap (10 M NaOH solution) between the jacketed reactor and gas burette. The gas generated during the reaction was passed through the NaOH trap and CO_2 was captured, leaving only H_2. The gas volume change observed before and after the NaOH trap experiment was used to quantify CO_2 and H_2.

2.2.5 General Procedure for Catalytic Formation of Primary Amines

Ar-NO_2 (1 mmol), $Ag_{48}Pd_{52}/WO_{2.72}$ (3 mol%), dioxane (6 mL) and water (3 mL) were stirred for 5 min in a 50 mL flask at 50.0 °C. Next, FA (4 mmol) was added to the reaction mixture, and the flask was sealed by a balloon. The solution was stirred at 800 rpm at 50.0 °C for a pre-set reaction time. The progress of the reaction and the yields of the amine compounds were determined by GC-MS with benzyl ether as an internal standard.

2.2.6 General Procedure for Catalytic One-Pot Synthesis of Benzoazoles

2-Nitrobenzene substrate (1 mmol), aldehyde (1.2 mmol), $Ag_{48}Pd_{52}/WO_{2.72}$ (3 mol%), dioxane (6 mL) and water (3 mL) were stirred for 5 min in a 25 mL flask at 80 °C. Next, FA (4 mmol) was added to the reaction mixture, and the flask was sealed by a balloon. The solution was stirred at 800 rpm at 80 °C for 8 h. After completion of the reaction, a small amount of ethyl acetate was added and the catalyst was removed by centrifugation at 9500 rpm and washed three times with water and methanol. Then the catalyst was dried before further use. The solvent was removed under vacuum and the residue was purified by column chromatography (hexane/ethyl acetate = 8:1) to give the product.

2.2.7 Characterization

Samples for transmission electron microscopy (TEM) and high-resolution TEM (HRTEM) analyses were prepared by depositing a single drop of diluted NP dispersion/suspension on amorphous-carbon-coated copper grids. Images were obtained by a JEOL 2010 TEM (200 kV). X-Ray powder diffraction (XRD) patterns of the samples were collected on a Bruker AXS D8-Advanced diffractometer with Cu Kα radiation (λ = 1.5406 Å). The compositions of the AgPd NPs and the molar ratio of AgPd/$WO_{2.72}$ were measured by inductively coupled plasma–atomic emission spectroscopy (ICP–AES). For ICP–AES analyses, the dried NPs were dissolved in warm aqua regia (~70 °C, 30 min) to ensure the complete dissolution of metal into the acid. The solution was then diluted with 2% HNO_3 solution. The measurements were carried out on a JY2000 Ultrace ICP–AES equipped with a JY-AS 421 auto sampler and 2400 g/mm holographic grating. TLC analysis was done using silica gel TLC with 60 F254 indicators. The analyses of the one-pot reaction products were carried out by GC-MS using an Agilent 6890 GC coupled to a 5973 Mass spectrometer detector with a DB-5 (Agilent) fused silica capillary column (L × I.D. 30 m × 0.25 mm, df 0.25 μm) and helium as carrier gas. The gas chromatograph was temperature programmed from 65 °C (3 min initial time) to 300 °C at 6 °C min^{-1} (isothermal for 20 min final time). The mass spectrometer was operated in the electron impact mode at 70 eV ionization energy. NMR spectra were recorded using a Bruker Avance III Ultra-Shield 400 MHz spectrometer (400 MHz for ^{1}H, 100 MHz for ^{13}C) at 296 K. Chemical shifts are reported in ppm relative to the residual solvent signal, coupling constants (J) are reported in Hz.
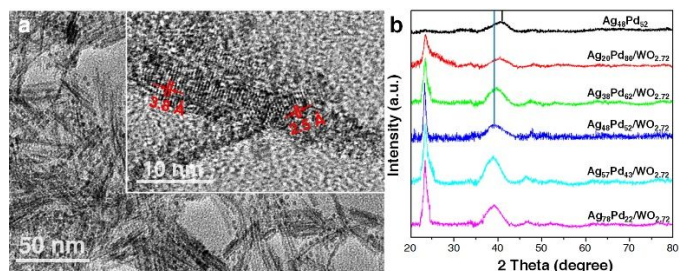
3 Results and discussion

Fig. 2 (a) TEM image of the $Ag_{48}Pd_{52}/WO_{2.72}$ nanocomposite. Inset: HRTEM image of $Ag_{48}Pd_{52}/WO_{2.72}$. (b) XRD pattern of the $Ag_{48}Pd_{52}/WO_{2.72}$ and $Ag_{48}Pd_{52}$ NPs synthesized without $WO_{2.72}$. Inset: XRD patterns of $Ag_{78}Pd_{22}/WO_{2.72}$, $Ag_{57}Pd_{43}/WO_{2.72}$, $Ag_{48}Pd_{52}/WO_{2.72}$, $Ag_{38}Pd_{61}/WO_{2.72}$ and $Ag_{20}Pd_{80}/WO_{2.72}$.

The AgPd/$WO_{2.72}$ catalyst contains AgPd NPs perched on $WO_{2.72}$ nanorods (NRs), as shown in Fig. 2a. $WO_{2.72}$ NRs were prepared by reacting WCl_4 with oleic acid (OA) and oleylamine (OAm) in 1-octadecene (ODE) at 280 °C,[37] while AgPd/$WO_{2.72}$ was obtained by growing AgPd NPs at 180 °C in the presence of the $WO_{2.72}$ NRs.[38] Under these reaction conditions, the molar ratios of Ag/Pd and the mass ratios of AgPd/$WO_{2.72}$ were controlled by varying the amounts of the Ag- and Pd-precursors and WCl_4, and were determined using inductively coupled plasma-atomic emission spectroscopy (ICP-AES). We prepared $Ag_{78}Pd_{22}/WO_{2.72}$, $Ag_{57}Pd_{43}/WO_{2.72}$, $Ag_{48}Pd_{52}/WO_{2.72}$, $Ag_{38}Pd_{61}/WO_{2.72}$ and $Ag_{20}Pd_{80}/WO_{2.72}$, with a fixed ratio of AgPd to $WO_{2.72}$ of 3:5 mol/mol. Representative TEM images of $Ag_{48}Pd_{52}/WO_{2.72}$ (Fig. 2a) show that the NPs have an average diameter of 2.3 ± 0.1 nm and "perch" on 40 × 5 nm $WO_{2.72}$ NRs. High-resolution TEM (HRTEM) images of the composite (Inset in Fig. 2a) show that the $WO_{2.72}$ NRs have a good crystalline structure with an interfringe distance of 3.8 Å, which corresponds to the (010) interplanar spacing of monoclinic $WO_{2.72}$ (3.78 Å, JCPDS NO. 65-1291). The $Ag_{48}Pd_{52}$ NPs attached to the $WO_{2.72}$ NRs have an interfringe distance of 2.5 Å, which is larger than (111) interplanar spacing of 2.3 Å observed for independent $Ag_{48}Pd_{52}$ NPs (Fig. S1†). X-ray diffraction (XRD) of the $Ag_{48}Pd_{52}$ NPs exhibit a wide (111) peak around 40° (Figure 2b). Once attached to $WO_{2.72}$, the (111) peak shifts to a smaller angle, indicating that AgPd NPs coupled to $WO_{2.72}$ have their lattice expanded. The (111) peaks of AgPd/$WO_{2.72}$ show Ag/Pd-composition-dependent shifts (Fig. 2b) and the corresponding lattice parameters lie along the theoretical line based on Vegard's law (Fig. S2†), confirming the formation of an alloy structure of AgPd, not a core/shell structure. As a comparison, $WO_{2.72}$ does not show obvious pattern changes. X-ray photoelectron spectroscopy (XPS) was further used to characterize the AgPd NPs, $WO_{2.72}$ NRs and the AgPd/$WO_{2.72}$ composite structure (Fig. 3a-b). Once attached to $WO_{2.72}$, the Ag 3d and Pd 3d binding energies of the AgPd NPs increase slightly. The Ag 3d peaks shift less (from 368.1/374.1 eV to 368.2/374.2 eV) than the Pd 3d ones (from 336.4/341.8 eV to 336.8/342.1 eV). In contrast, the binding energy of W 4f in the composite structure is down-shifted (Fig. 3c). These observations indicate that the electron density of AgPd is decreased in the composite

structure, and that Pd is affected more than Ag by the AgPd-$WO_{2.72}$ interactions.[37, 39-43]

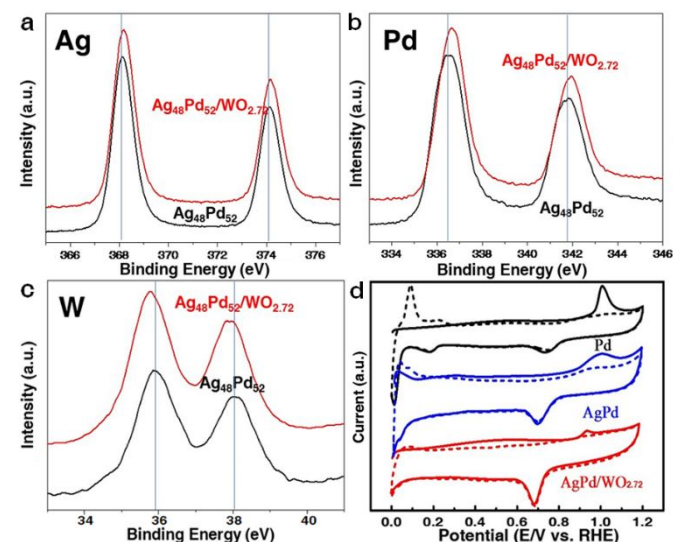**Fig. 3** (a-c) XPS spectra of $Ag_{48}Pd_{52}/WO_{2.72}$ and $Ag_{48}Pd_{52}$ (Ag 3d, Pd 3d and W 4f). (d) CO stripping voltammetry of the $Ag_{48}Pd_{52}/WO_{2.72}$ composites, $Ag_{48}Pd_{52}$ and commercial Pd obtained in 0.1 M $HClO_4$ with a scan rate of 20 mV/s. The solid line is from the first scanning cycle and the dashed line is from the second scanning cycle.

The interaction between AgPd and $WO_{2.72}$ induces charge polarization from AgPd to $WO_{2.72}$, which should increase the Lewis acidity of the AgPd NP, and the Lewis basicity of $WO_{2.72}$, facilitating AgPd binding of electrons and $WO_{2.72}$ absorption of protons. We first studied the CO binding properties of the AgPd surface via the CO stripping test (Fig. 3d). From Pd to AgPd, the CO stripping peak is negatively shifted and broadened, indicating that CO is oxidized more easily on the AgPd surface than on the Pd surface. Once coupled with $WO_{2.72}$, the CO stripping peak is much weaker and more negatively shifted, demonstrating the improved CO-tolerance on the AgPd surface. We then evaluated the catalytic properties of AgPd/$WO_{2.72}$ for formic acid (FA) dehydrogenation. We found that the conditions, previously optimized in aqueous solution (10 mL of 900 mM FA, 323 K), were still suitable for the current catalyst system. Gas chromatography (GC) analyses (Fig. S3†) show that the gas mixture consists of only CO_2 and H_2, and no CO is present. Using a NaOH trap to remove CO_2 from the gas mixture, we obtained the H_2 volume (Fig. S4†). Our studies show that AgPd/$WO_{2.72}$ catalyzes FA decomposition in a CO-free pathway, and that the strong AgPd-$WO_{2.72}$ interaction makes AgPd more electrophilic, favoring the activation of FA to generate HCOO* via O–H bond cleavage or *COOH via C–H bond cleavage.[27, 40-49] CO_2 and H_2 are formed via the AgPd-promoted decomposition of HCOO* and *COOH, which essentially blocks the CO-forming pathway.

$Ag_{48}Pd_{52}$-catalyzed dehydrogenation of FA was evaluated at 323 K with [AgPd] = 3.1 mM. Fig. 4a and Fig. S5† show that 3/5 molar ratio and 900 mM are necessary to reach optimum catalytic activity. Adding more $Ag_{48}Pd_{52}$ and $WO_{2.72}$ does not lead to the continued increase of TOF, rather it decreases its value due to apparent over-loading of the catalyst. At [FA] = 900 mM and [AgPd]/$WO_{2.72}$ = 3/5 mol/mol, it shows the best activity

with a TOF value reaching 1718 h^{-1}. This TOF is among the highest ever reported for Pd-based catalysts (Table S1†).[29,50-56] We also tested the effects of different inorganic supports, such as conventional carbon (C), silica (SiO$_2$), graphene (G), or commercial WO$_3$ and WO$_{2.9}$ on the Ag$_{48}$Pd$_{52}$ catalysis at the 3/5 [AgPd]/[support] ratios (Fig. 4b). These composites are all less active than Ag$_{48}$Pd$_{52}$/WO$_{2.72}$, suggesting that AgPd coupling to WO$_{2.72}$ favors the dehydrogenation of FA.

Ag$_{48}$Pd$_{52}$/WO$_{2.72}$ could further catalyze transfer hydrogenation from HCOOH to R-NO$_2$ to give R-NH$_2$ at 50 °C. Using nitrobenzene as a model substrate, we optimized the reaction conditions: 1 mmol nitrobenzene, 3.0 mmol FA, 3 mol% Ag$_{48}$Pd$_{52}$/WO$_{2.72}$ in 9 mL H$_2$O/dioxane (1:2 v/v). Under these conditions the dehydrogenation of FA and hydrogenation of nitrobenzene were complete within 30 mins, and aniline was isolated in a 98% yield. Using similar reaction conditions, a variety of substituted nitrobenzene derivatives could be reduced to the corresponding anilines in yields above 90% within 2 h (Table S2†). Ag/Pd-dependent studies indicate that Ag$_{48}$Pd$_{52}$/WO$_{2.72}$ is the best catalyst for FA dehydrogenation, and transfer hydrogenation to reduce nitro groups (Fig. S6†).
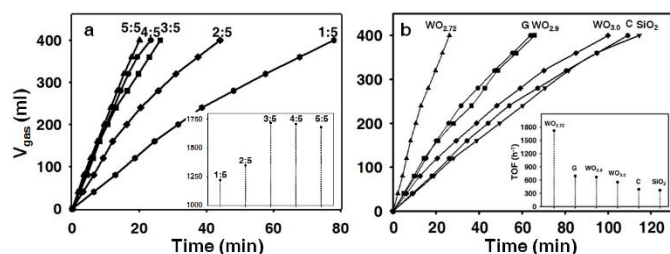

Fig. 4 (a) Plot of time vs volume of gas generated from FA dehydrogenation catalyzed by nanocomposites with different Ag$_{48}$Pd$_{52}$/WO$_{2.72}$ molar ratio ([AgPd] = 3.1 mM, [FA] = 900 mM, T = 323 K). Inset: The dehydrogenation TOF values of nanocomposites with different Ag$_{48}$Pd$_{52}$/WO$_{2.72}$ molar ratios. (b) Plot of time vs. volume of gas generated from FA dehydrogenation catalyzed by Ag$_{48}$Pd$_{52}$ on different supports ([AgPd] = 3.1 mM, [FA] = 900 mM, T = 323 K). Inset: TOF values of Ag$_{48}$Pd$_{52}$ on different supports.

We further extended this reaction to a one-pot synthesis of benzoxazoles (Table 1) starting from 2-nitrophenol and an aldehyde. Various benzoxazoles (entries **1-8**) were obtained in >90% yield at 80 °C within 8 h. The electronic properties of substituents at either the para- or meta-positions of the benzaldehyde had little influence on the reaction outcome. However, substituents at the ortho position decreased the yield somewhat (entries **9-10**), likely due to steric hindrance. The good yield (91%) of the thiophene derivative (entry **11**) shows that the reaction is tolerant to substrates containing a sulfur atom. However, replacing the aromatic aldehyde with an aliphatic aldehyde does lower the yield (entry **12**).

Table 1. Ag$_{48}$Pd$_{52}$/WO$_{2.72}$-catalyzed one-pot condensation of 2-nitrophenol with various aldehydes.[a]
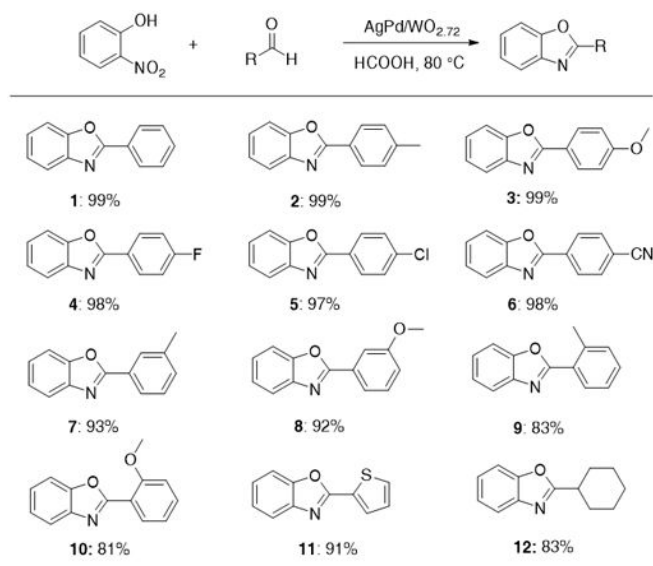
[a] Reaction conditions: 2-nitrophenol (1 mmol), aldehyde (1.2 mmol), Ag$_{48}$Pd$_{52}$/WO$_{2.72}$ (3 mol%), dioxane (6 mL), water (3 mL) and FA (4 mmol), 8 h.

To determine if other steps in this multi-step reaction, in addition to FA dehydrogenation and reduction of the nitro group, were dependent on the structure and composition of the catalyst, we examined the synthesis of 2-phenylbenzoxazole starting from 2-aminophenol and benzaldehyde. The reaction was performed using the same conditions as shown in Table 1, and we used GC-MS to monitor the concentrations of the 2-aminophenol starting material, the imine intermediate, and the benzoxazole product. The most efficient catalyst for synthesis of 2-phenylbenzoxazole starting from 2-aminophenol is Ag$_{48}$Pd$_{52}$/WO$_{2.72}$ (Fig. 5a). 2-Aminophenol was almost completely consumed after 3 h, and the reaction was essentially complete after 7 h. Fig. 5b shows the accumulation and subsequent consumption of the imine intermediate (black circles) formed by dehydration of the amino group of 2-aminophenol with benzaldehyde. This intermediate quickly accumulates during the first two hours of the reaction, before it is transformed more slowly to the product. Other AgPd-catalysts were not as efficient as Ag$_{48}$Pd$_{52}$/WO$_{2.72}$ for both the condensation of 2-aminophenol and benzaldehyde to give the imine intermediate, and also the cyclization and dehydrogenation of the intermediate to give the final benzoxazole product. Among the catalysts studied, Ag is the least active catalyst for both of these processes. Taken together, these synthetic data indicate that; 1) FA dehydrogenation, transfer hydrogenation from Ar-NO$_2$ to Ar-NH$_2$, and Ar-NH$_2$ reaction with aldehydes to form benzoxazoles are all dependent on the AgPd composition and identity of the solid support of the catalyst, 2) Ag$_{48}$Pd$_{52}$/WO$_{2.72}$ is the most effective catalyst for all of these reaction steps, and 3) the reactions are not significantly affected by the electronic character of substituents on the aldehyde, but are influenced by the steric characteristics of the aldehyde.

The Ag$_{48}$Pd$_{52}$/WO$_{2.72}$ catalyst was not only active, but also stable under the one-pot reaction conditions. For example, in the formation of 2-phenylbenzoxazole, after the reaction was

complete the catalyst was precipitated by adding ethyl acetate, isolated and purified by washing with water/methanol, and re-used. After 5 rounds of catalyst reuse, the catalyst showed little drop in activity, and the yield of the final product remained above 95% for all five reactions. In addition, the catalyst showed no obvious changes in morphology (Fig. S7†).
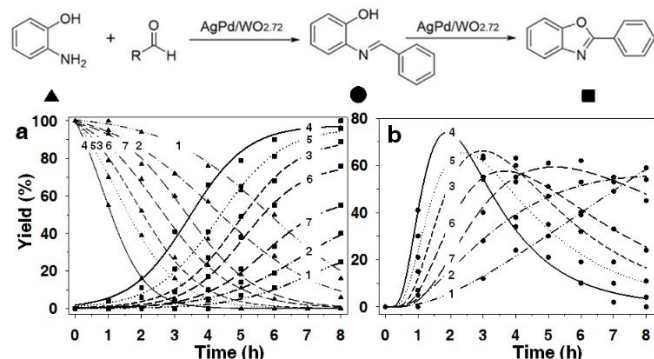

Fig. 5 $Ag_xPd_y/WO_{2.72}$-catalyzed condensation of 2-aminophenol and benzaldehyde. (a) Time-dependent formation of 2-phenylbenzoxazole (rectangles) starting from 2-aminophenol (triangles). (b) Time-dependent formation and consumption of the imine intermediate (circles). Note: (1) Ag, (2) $Ag_{78}Pd_{22}$, (3) $Ag_{57}Pd_{43}$, (4) $Ag_{48}Pd_{52}$, (5) $Ag_{39}Pd_{61}$, (6) $Ag_{20}Pd_{80}$ and (7) Pd.
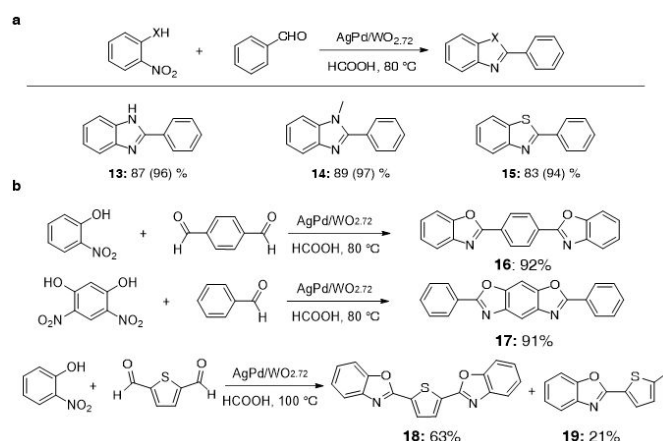

Fig. 6 (a) $Ag_{48}Pd_{52}/WO_{2.72}$-catalyzed synthesis of 2-phenylbenzimidazole, 1-methyl-2-phenylbenzimidazole and 2-phenylbenzothiazole. Reaction conditions: substrate (1 mmol), benzaldehyde (1.2 mmol), $Ag_{48}Pd_{52}/WO_{2.72}$ (3 mol%), dioxane (6 mL), water (3 mL) and FA (4 mmol), 8 h. The yields in parentheses were obtained at 90 °C. (b) $Ag_{48}Pd_{52}/WO_{2.72}$-catalyzed synthesis of phenylene-bis-benzoxazole, 2,6-diphenyl-benzobis(oxazole) and 2,5-bis(benzoxazol-2-yl)thiophene.

The AgPd/WO$_{2.72}$ catalyzed one-pot reaction was not limited to the formation of benzoxazoles, but could also be extended to the synthesis of other benzene-fused heterocycles (Fig. 6). By replacing 2-nitrophenol with 2-nitroaniline, *N*-methyl-2-nitroaniline or 2-nitrothiophenol, we obtained the corresponding benzimidazoles or benzothiazole in >83% yield using the same one-pot reaction conditions (**13-15**). By raising the reaction temperature from 80 to 90 °C, the yields were further improved to >94% (**13-15** in parentheses). It is notable that the yield of 2-phenylbenzothiazole remains high at 94%. The AgPd/WO$_{2.72}$ catalyst is not negatively affected by the thiol group in the 2-nitrothiophenol starting material. This outcome is different than what has been reported previously for other

Pd-based nanocatalysts, which are typically poisoned by thiols.[57-60] This observation suggests that the presence of the WO$_{2.72}$ helps to protect the AgPd catalyst from poisoning.

The one-pot reaction could be further extended to prepare phenylene-bis-benzoxazole (**16**) and 2,6-diphenyl-benzobis(oxazole) (**17**) from 2-nitrophenol/terephthalaldehyde and 4,6-dinitroresorcinol/benzaldehyde under the same 80 °C reaction conditions with >90% yields, making the reaction very promising for fabricating linear π-conjugated polymers (work in progress). By elevating the temperature to 100 °C, the reaction was also suitable for condensation of two equivalents of 2-nitrophenol with thiophene-2,5-dicarbaldehyde to give 2,5-bis(benzoxazol-2-yl)thiophene (**18**) (Fig. S8†), the known commercial fluorescent brightener 185. This brightener is normally prepared from the reaction between 2-aminophenol and thiophene-2,5-dicarboxylic acid in toluene and *N*-methyl-2-pyrrolidone at 185 °C with boric acid as an additive.[61] Compared with this conventional approach, our one-pot reaction is milder and produces the brightener in a modestly good yield. This 63% yield is somewhat lower than what we have observed for the other reactions reported herein. This reduced yield is not due to poisoning of the catalyst by the sulfur atom of thiophene. Rather, it is caused by reduction of one of the aldehyde groups in thiophene-2,5-dicarbaldehyde to the corresponding methyl group. During synthesis of *bis*-benzoxazole **18**, we also observe formation of the byproduct compound **19** in 21% yield. The study of this reduction of thiophene aldehyde is out of the scope of this paper and will be investigated separately.

Conclusions

In this article, we studied extensively on the AgPd/WO$_{2.72}$ catalysis and its general use for the one-pot syntheses of benzene-fused heterocyclic compounds. Our studies first examined the WO$_{2.72}$ NR-mediated growth of AgPd NPs resulting in the formation of AgPd/WO$_{2.72}$ composites. The interfacial interaction between AgPd and WO$_{2.72}$ leads to the desired alloy NP lattice expansion and charge polarization from AgPd to WO$_{2.72}$. This interaction enhances the AgPd/WO$_{2.72}$ catalysis of FA dehydrogenation at a temperature of 50 °C, TOF = 1718/h, E_a = 31 kJ/mol. The dehydrogenation reaction is Ag/Pd dependent, and $Ag_{48}Pd_{52}/WO_{2.72}$ is found to be the most active catalyst to produce H_2 and CO_2 via a pathway that does not produce CO. The power of the AgPd/WO$_{2.72}$ catalyst is further demonstrated by the transfer hydrogenation from FA to Ar-NO$_2$ to give Ar-NH$_2$ at 50 °C, and to the reaction of Ar-NH$_2$ with an aldehyde at 80-90 °C to yield benzoxazoles. In the one-pot synthesis of benzoxazoles, the catalysis is not affected by the electronic character of substituents on the aldehyde, but is sensitive to steric hinderance on the aldehyde. In addition, the one-pot reaction can be extended to prepare various benzoazoles with the 5-member rings containing C-O, C-NH, or C-S bonds. The AgPd/WO$_{2.72}$-catalyzed one-pot reaction offers a general approach to benzene-fused heterocyclic compounds for pharmaceutical and functional polymer applications.

Conflicts of interest

There are no conflicts of interest to declare.

Acknowledgements

Notes and references

1   T. Ghosh and M. Lehmann, *J. Mater. Chem. C*, 2017, **5**, 12308-12337.
2   S. Noel, S. Cadet, E. Gras and C. Hureau, *Chem. Soc. Rev.*, 2013, **42**, 7747-7762.
3   K. Amaike, K. Muto, J. Yamaguchi and K. Itami, *J Am Chem Soc*, 2012, **134**, 13573-13576.
4   W. Ai, W. W. Zhou, Z. Z. Du, Y. P. Du, H. Zhang, X. T. Jia, L. H. Xie, M. D. Yi, T. Yu and W. Huang, *J. Mater. Chem.*, 2012, **22**, 23439-23446.
5   J. S. Wu, W. M. Liu, J. C. Ge, H. Y. Zhang and P. F. Wang, *Chem. Soc. Rev.*, 2011, **40**, 3483-3495.
6   M. G. Rabbani, T. Islamoglu and H. M. El-Kaderi, *J. Mater. Chem. A*, 2017, **5**, 258-265.
7   S. J. Luo, J. Y. Liu, H. Q. Lin, B. A. Kazanowska, M. D. Hunckler, R. K. Roeder and R. L. Guo, *J. Mater. Chem. A*, 2016, **4**, 17050-17062.
8   X. M. Hao, J. Zhu, X. Jiang, H. T. Wu, J. S. Qiao, W. Sun, Z. H. Wang and K. N. Sun, *Nano Lett.*, 2016, **16**, 2981-2987.
9   K. Zhang, J. Liu and H. Ishida, *Macromolecules*, 2014, **47**, 8674-8681.
10 L. Tang, X. F. Guo, Y. Yang, Z. G. Zha and Z. Y. Wang, *Chem. Commun.*, 2014, **50**, 6145-6148.
11 A. Khalafi-Nezhad and F. Panahi, *Acs Catal.*, 2014, **4**, 1686-1692.
12 X. X. Cao, X. F. Cheng, Y. Bai, S. W. Liu and G. J. Deng, *Green Chem.*, 2014, **16**, 4644-4648.
13 X. K. Jin, Y. X. Liu, Q. Q. Lu, D. J. Yang, J. K. Sun, S. S. Qin, J. W. Zhang, J. X. Shen, C. H. Chu and R. H. Liu, *Org. Biomol. Chem.*, 2013, **11**, 3776-3780.
14 M. Y. Wu, X. Hu, J. Liu, Y. F. Liao and G. J. Deng, *Org. Lett.*, 2012, **14**, 2722-2725.
15 E. Gianotti, M. Taillades-Jacquin, J. Rozière and D. J. Jones, *Acs Catal.*, 2018, **8**, 4660-4680.
16 K. Sordakis, C. H. Tang, L. K. Vogt, H. Junge, P. J. Dyson, M. Beller and G. Laurenczy, *Chem. Rev.*, 2018, **118**, 372-433.
17 Z. Lu, V. Cherepakhin, I. Demianets, P. J. Lauridsen and T. J. Williams, *Chem. Commun.*, 2018, DOI: 10.1039/c8cc03412e.
18 Y. B. Shen, Y. L. Zhan, S. P. Li, F. D. Ning, Y. Du, Y. J. Huang, T. He and X. C. Zhou, *Chem. Sci.*, 2017, **8**, 7498-7504.
19 Z. Shiwei, Y. Fusheng, Z. Lu, Z. Yang, W. Zhen, Z. Zaoxiao and W. Yuqi, *Int. J. Energy Res.*, **42**, 3837-3850.
20 S. J. Li, Y. Ping, J. M. Yan, H. L. Wang, M. Wu and Q. Jiang, *J. Mater. Chem. A*, 2015, **3**, 14535-14538.
21 Q. L. Zhu, F. Z. Song, Q. J. Wang, N. Tsumori, Y. Himeda, T. Autrey and Q. Xu, *J. Mater. Chem. A*, 2018, **6**, 5544-5549.
22 W. H. Zhong, Y. X. Liu, M. S. Deng, Y. C. Zhang, C. Y. Jia, O. V. Prezhdo, J. Y. Yuan and J. Jiang, *J. Mater. Chem. A*, 2018, **6**, 11105-11112.
23 J. Song, X. J. Gu, J. Cheng, N. Fan, H. Zhang and H. Q. Su, *Appl Catal B-Environ*, 2018, **225**, 424-432.
24 H. Liu, B. L. Huang, J. H. Zhou, K. Wang, Y. S. Yu, W. W. Yang and S. J. Guo, *J. Mater. Chem. A*, 2018, **6**, 1979-1984.
25 X. F. Guo, C. Yu, Z. Y. Yin, S. H. Sun and C. T. Seto, *Chemsuschem*, 2018, **11**, 1617-1620.
26 C. Yu, X. Guo, M. Shen, B. Shen, M. Muzzio, Z. Yin, Q. Li, Z. Xi, J. Li, C. T. Seto and S. Sun, *Angew. Chem. Int. Ed.*, 2017, **139**, 5712-5715.
27 L. P. Xiao, Y. S. Jun, B. H. Wu, D. Y. Liu, T. T. Chuong, F. A. Jie and G. D. Stucky, *J. Mater. Chem. A*, 2017, **5**, 6382-6387.
28 Q. M. Sun, N. Wang, Q. M. Bing, R. Si, J. Y. Liu, R. S. Bai, P. Zhang, M. J. Jia and J. H. Yu, *Chem*, 2017, **3**, 477-493.
29 J. Cheng, X. J. Gu, P. L. Liu, H. Zhang, L. L. Ma and H. Q. Su, *Appl Catal B-Environ*, 2017, **218**, 460-469.
30 S. Jo, P. Verma, Y. Kuwahara, K. Mori, W. Choi and H. Yamashita, *J. Mater. Chem. A*, 2017, **5**, 21883-21892.

31 H. Liu, X. Y. Liu, Y. S. Yu, W. W. Yang, J. Li, M. Feng and H. B. Li, *J. Mater. Chem. A*, 2018, **6**, 4611-4616.

32 C. Yu, X. F. Guo, Z. Xi, M. Muzzio, Z. Y. Yin, B. Shen, J. R. Li, C. T. Seto and S. H. Sun, *J Am Chem Soc*, 2017, **139**, 5712-5715.

33 Q. Zhang, S. S. Li, M. M. Zhu, Y. M. Liu, H. Y. He and Y. Cao, *Green Chem.*, 2016, **18**, 2507-2513.

34 R. V. Jagadeesh, D. Banerjee, P. B. Arockiam, H. Junge, K. Junge, M. M. Pohl, J. Radnik, A. Bruckner and M. Beller, *Green Chem.*, 2015, **17**, 898-902.

35 R. Javaid, S. Kawasaki, A. Suzuki and T. M. Suzuki, *Beilstein J. Org. Chem.*, 2013, **9**, 1156-1163.

36 C. Jouannin, I. Dez, A. C. Gaumont, J. M. Taulemesse, T. Vincent and E. Guibal, *Appl. Catal. B Environ.*, 2011, **103**, 444-452.

37 Z. Xi, D. P. Erdosy, A. Mendoza-Garcia, P. N. Duchesne, J. R. Li, M. Muzzio, Q. Li, P. Zhang and S. H. Sun, *Nano Lett.*, 2017, **17**, 2727-2731.

38 S. Zhang, O. Metin, D. Su and S. H. Sun, *Angew. Chem. Int. Ed.*, 2013, **52**, 3681-3684.

39 H. Y. Wang, R. X. Fan, J. Y. Miao, J. Y. Chen, S. J. Mao, J. Deng and Y. Wang, *J. Mater. Chem. A*, 2018, **6**, 6780-6784.

40 H. F. Cheng, M. Klapproth, A. Sagaltchik, S. Li and A. Thomas, *J. Mater. Chem. A*, 2018, **6**, 2249-2256.

41 A. Martinez-Garcia, V. K. Vendra, S. Sunkara, P. Haldankar, J. Jasinski and M. K. Sunkara, *J. Mater. Chem. A*, 2013, **1**, 15235-15241.

42 C. H. Kuo, L. K. Lamontagne, C. N. Brodsky, L. Y. Chou, J. Zhuang, B. T. Sneed, M. K. Sheehan and C. K. Tsung, *Chemsuschem*, 2013, **6**, 1993-2000.

43 H. Bai, N. Su, W. T. Li, X. Zhang, Y. Yan, P. Li, S. X. Ouyang, J. H. Ye and G. C. Xi, *J. Mater. Chem. A*, 2013, **1**, 6125-6129.

44 M. Tsuji, D. Shimamoto, K. Uto, M. Hattori and H. Ago, *J. Mater. Chem. A*, 2016, **4**, 14649-14656.

45 Y. Q. Jiang, X. L. Fan, X. Z. Xiao, T. Qin, L. T. Zhang, F. L. Jiang, M. Li, S. Q. Li, H. W. Ge and L. X. Chen, *J. Mater. Chem. A*, 2016, **4**, 657-666.

46 R. B. N. Baig, S. Verma, M. N. Nadagouda and R. S. Varma, *Green Chem.*, 2016, **18**, 1019-1022.

47 J. J. Song, Z. F. Huang, L. Pan, J. J. Zou, X. W. Zhang and L. Wang, *Acs Catal.*, 2015, **5**, 6594-6599.

48 Y. Ping, J. M. Yan, Z. L. Wang, H. L. Wang and Q. Jiang, *J. Mater. Chem. A*, 2014, **2**, 13745-13745.

49 S. Yamazoe, Y. Masutani, K. Teramura, Y. Hitomi, T. Shishido and T. Tanaka, *Appl. Catal. B Environ.*, 2008, **83**, 123-130.

50 H. Zhong, M. Iguchi, F. Z. Song, M. Chatterjee, T. Ishizaka, I. Nagao, Q. Xu and H. Kawanami, *Sustain. Energ. Fuels*, 2017, **1**, 1049-1055.

51 H. J. Jeon and Y. M. Chung, *Appl. Catal. B Environ.*, 2017, **210**, 212-222.

52 X. C. Yang, P. Pachfule, Y. Chen, N. Tsumori and Q. Xu, *Chem. Commun.*, 2016, **52**, 4171-4174.

53 J. Cheng, X. J. Gu, X. L. Sheng, P. L. Liu and H. Q. Su, *J. Mater. Chem. A*, 2016, **4**, 1887-1894.

54 J. Cheng, X. J. Gu, P. L. Liu, T. S. Wang and H. Q. Su, *J. Mater. Chem. A*, 2016, **4**, 16645-16652.

55 Q. Y. Bi, J. D. Lin, Y. M. Liu, H. Y. He, F. Q. Huang and Y. Cao, *Angew Chem Int Edit*, 2016, **55**, 11849-11853.

56 J. H. Lee, J. Cho, M. Jeon, M. Ridwan, H. S. Park, S. H. Choi, S. W. Nam, J. Han, T. H. Lim, H. C. Ham and C. W. Yoon, *J. Mater. Chem. A*, 2016, **4**, 14141-14147.

57 Z. X. Luo, A. W. Castleman and S. N. Khanna, *Chem. Rev.*, 2016, **116**, 14456-14492.

58 B. L. Xu, G. Gonella, B. G. DeLacy and H. L. Dai, *J. Phys. Chem. C*, 2015, **119**, 5454-5461.

59 M. Moreno, F. J. Ibanez, J. B. Jasinski and F. P. Zamborini, *J. Am. Chem. Soc.*, 2011, **133**, 4389-4397.

60 J. C. Garcia-Martinez, R. W. J. Scott and R. M. Crooks, *J. Am. Chem. Soc.*, 2003, **125**, 11190-11191.

61 V. Eliu and J. Hauser, *U.S. Patent Application*, 2003, US20070249840A1.

Table of contents (TOC) figure

One-Pot Formic Acid Dehydrogenation and Synthesis of Benzene-fused Heterocycles over Reusable AgPd/WO$_{2.72}$ Nanocatalyst†

Chao Yu,[‡a] Xuefeng Guo,[‡a] Bo Shen,[a] Zheng Xi,[a] Qing Li,[b] Zhouyang Yin,[a] Hu Liu,[a] Michelle Muzzio,[a] Mengqi Shen,[a] Junrui Li,[a] Christopher T. Seto*[a] and Shouheng Sun*[a]

Nanocatalyst with AgPd nanoparticles coupled to WO$_{2.72}$ nanorods combines multi-step reactions in one-pot to prepare complex heterocycles under mild conditions.